Substrate Degradation Kinetics, Microbial Diversity, and Current Efficiency of Microbial Fuel Cells Supplied with Marine Plankton[∇]

Clare E. Reimers,[1]* Hilmar A. Stecher III,[1] John C. Westall,[2] Yvan Alleau,[1] Kate A. Howell,[1] Leslie Soule,[1] Helen K. White,[3] and Peter R. Girguis[3]

College of Oceanic and Atmospheric Sciences, Hatfield Marine Science Center, Oregon State University, Newport, Oregon 97365[1]; Department of Chemistry, Oregon State University, 153 Gilbert Hall, Corvallis, Oregon 97331[2]; and Harvard University, Biological Labs, 16 Divinity Avenue, Cambridge, Massachusetts 02138[3]

The decomposition of marine plankton in two-chamber, seawater-filled microbial fuel cells (MFCs) has been investigated and related to resulting chemical changes, electrode potentials, current efficiencies, and microbial diversity. Six experiments were run at various discharge potentials, and a seventh served as an open-circuit control. The plankton consisted of a mixture of freshly captured phytoplankton and zooplankton (0.21 to 1 mm) added at an initial batch concentration of 27.5 mmol liter^{-1} particulate organic carbon (OC). After 56.7 days, between 19.6 and 22.2% of the initial OC remained, sulfate reduction coupled to OC oxidation accounted for the majority of the OC that was degraded, and current efficiencies (of the active MFCs) were between 11.3 and 15.5%. In the open-circuit control cell, anaerobic plankton decomposition (as quantified by the decrease in total OC) could be modeled by three terms: two first-order reaction rate expressions (0.79 day^{-1} and 0.037 day^{-1}, at 15°C) and one constant, no-reaction term (representing 10.6% of the initial OC). However, in each active MFC, decomposition rates increased during the third week, lagging just behind periods of peak electricity generation. We interpret these decomposition rate changes to have been due primarily to the metabolic activity of sulfur-reducing microorganisms at the anode, a finding consistent with the electrochemical oxidization of sulfide to elemental sulfur and the elimination of inhibitory effects of dissolved sulfide. Representative phylotypes, found to be associated with anodes, were allied with *Delta-*, *Epsilon-*, and *Gammaproteobacteria* as well as the *Flavobacterium-Cytophaga-Bacteroides* and *Fusobacteria*. Based upon these results, we posit that higher current efficiencies can be achieved by optimizing plankton-fed MFCs for direct electron transfer from organic matter to electrodes, including microbial precolonization of high-surface-area electrodes and pulsed flowthrough additions of biomass.

Microbial fuel cells (MFCs) are devices that rely on microbial catabolism at an anode and the reduction of a terminal electron acceptor, preferably oxygen, at a cathode to convert biomass into electrical energy. One measure of the efficiency of these cells is the current efficiency (also known as coulombic efficiency), which is the percentage of electrons coming from oxidation of the organic fuel that ultimately are transferred as current (3, 30). MFCs fueled with simple substrates such as glucose, sucrose, and acetate (21, 38, 39) typically exhibit higher efficiencies than those fueled by more complex domestic wastes (18, 27). Two reasons for low efficiencies of microbial electricity production are (i) the resistance of some organic fractions to microbial degradation and (ii) the conversion of other organic fractions to degradation products or microbial biomass without electrons being passed to the fuel cell (13). Each new MFC construction, microbial culture, and/or source of biofuel requires assessment of potential losses. Seafloor and other underwater MFCs are new varieties receiving increased attention as promising power sources for autonomous sensors,

beacons, and communication devices for ocean monitoring and navigation (42, 43, 45, 48). These devices rely on marine plankton as their essential biofuel, but their current efficiencies have not been evaluated.

In the ocean, dissolved and particulate organic matter derived from phytoplankton and zooplankton biomass constitutes roughly 1,000 Pg of carbon that is renewed at a rate of 11 to 16 Pg year^{-1} (11). The biological respiration of marine organic matter is commonly expressed by the equation $(CH_2O)_\alpha(NH_3)_\beta(H_3PO_4) + \gamma O_2 \rightarrow \alpha CO_2 + \beta HNO_3 + H_3PO_4 + (\alpha + \beta)H_2O$, where organic carbon (OC) is assumed for simplicity to have thermodynamic properties similar to those of glucose or sucrose (14). The coefficients α, β, and γ are known as "Redfield ratios," and they are often assigned the values 106, 16, and 138, respectively, based on the findings of A. G. Redfield (2, 41). However, not all organic matter derived from marine plankton is readily metabolizable, and Redfield ratios may shift as organic material undergoes progressive stages of decomposition (47). Furthermore, reaction rates and the quantity of material degraded can be significantly greater under oxic as opposed to anoxic conditions (17, 49).

We were interested in determining how the redox-dependent susceptibility of marine organic materials to bacterial decomposition would be manifest under the unique biogeochemical conditions within an MFC. We were also interested

* Corresponding author. Mailing address: College of Oceanic and Atmospheric Sciences, Hatfield Marine Science Center, Oregon State University, Newport, OR 97365. Phone: (541) 867-0220. Fax: (541) 867-0138. E-mail: creimers@coas.oregonstate.edu.
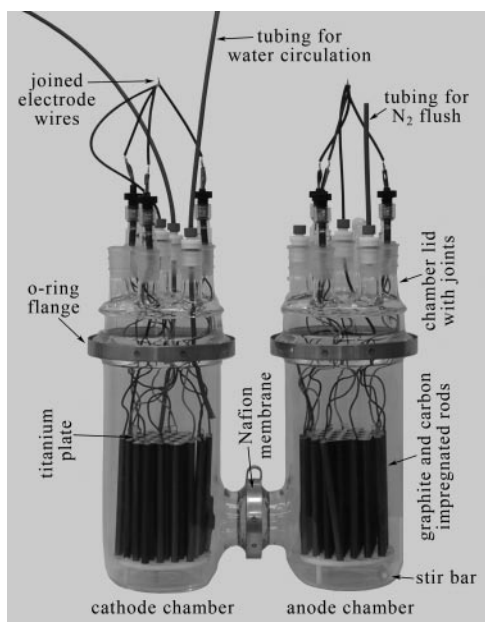
FIG. 1. Major components of the two-chamber MFCs. The Nafion membrane is not visible but is under the clamp as indicated in the picture.

FIG. 2. Experimental setup of MFC assemblies, with anode chambers to the left on stir plates and cathode chambers to the right on laboratory jacks.

in determining the relationships between plankton decomposition, microbial diversity, and energy production. We reasoned that within the confines of an anode chamber, organic substrates may be oxidized by either (i) microorganisms such as *Shewanella* or *Geobacter sulfurreducens* (5, 25, 31), which transfer electrons directly to electrodes, or (ii) fermentative and heterotrophic microorganisms that use dissolved electron acceptors other than oxygen. The former processes are akin thermodynamically to environmentally coupled suboxic and oxic biogeochemical reactions (e.g., those affecting Mn [1]), whereas the latter processes are purely anaerobic pathways, which typically are dominated by bacterial sulfate reduction in anoxic marine systems. In addition, sulfate reduction leads to the generation of sulfide, which is electrochemically active and may contribute to fuel cell power output (21, 40, 42, 45). Thus, the role of sulfide in determining current efficiencies was also a question.

To evaluate the oxidation of marine plankton-derived organic matter and the dependence of power generation on MFC parameters related to electric potential and duration of discharge, we conducted batch-fed MFC experiments in which the consumption of dissolved OC (DOC) and particulate OC (POC) fractions were quantified over time together with degradation end products and power output. The MFCs were designed as two-chamber systems with carbon anodes and cathodes of equal area. Cultured bacteria were not introduced into the fuel cells, but instead microbial communities were allowed to develop from the seawater medium and plankton additions.

As shown below, these experiments revealed that the decomposition rate of planktonic organic matter in an MFC is enhanced by the presence of the anode as an electron acceptor and that periods of enhanced degradation follow closely intervals of sulfide removal and peaks in power generation. Micro-

bial phylotypes recovered at the end points of three different treatments were allied to groups known to be involved in OC degradation and sulfur metabolism (as well as groups previously observed on MFC anodes). Interestingly, only minor qualitative changes in microbial community composition and diversity were observed between cells held at different potentials.

MATERIALS AND METHODS

MFC assemblies. Seven custom two-chamber, H-shape MFCs were assembled for this study from pairs of flat-bottom, 5-liter cylindrical flasks topped with 152 mm-inner-diameter (ID) Schott O-ring flanges (Ace Glass, Inc., Vineland, NJ). As shown in Fig. 1, the chambers were connected through side tubes leading to 60 mm-ID Schott O-ring flanges that were clamped against a Nafion 117 membrane (0.18 mm thick, product 274674; Aldrich, St. Louis, MO) and a CAPFE O ring (silicone O ring encapsulated in Teflon). Custom lids were produced with flat-bottom flanges from Ace Glass 152-mm-ID no. 6529 reactor heads. Each lid had one central- and six side-neck ground glass joints. During experiments, plugs or adapters were fitted to these joint openings, and the adapters were used to pass through wires, tubing, reference electrodes, or sensors of different types (see below). Temporary removal of the plugs or adapters permitted rapid chemical and biological sampling.

Each MFC electrode (anode or cathode) was constructed from 19 graphite and 18 glassy carbon-impregnated graphite rods (152 mm long by 9.5 mm outer diameter; Graphite Engineering and Sales, Greenville, MI, and Graphite Die Mold Inc., Durham, CT) equally spaced in a hexagonal array. The two grades of carbon substrate were utilized to assess possible surface property influences on microorganisms colonizing electrodes. Twenty-seven of the rods were fixed with nylon screws between a 0.089-mm-thick titanium (CP grade) plate at the top and a 6.4-mm-thick Delrin plate at the bottom. To aid water circulation, top and bottom plates were drilled with a honeycomb pattern of open holes. Water circulation was also facilitated by elevating the anode and cathode assemblies with three 25.4-mm-long standoffs. The titanium plate provided electrical conductance between the fixed rods, and it was joined to the end of a 64-cm-long section of neoprene-coated 20-gauge wire (1N2T; Pittsburgh Wire and Cable; Pittsburgh, PA) with silver-epoxy (Tiga Silver 901) that was overcoated with waterproof epoxy (West System Inc., Bay City, MI). Five additional pairs of rods (with one of each pair being graphite and the other glassy carbon-impregnated graphite) were individually wired and epoxy potted at their upper ends so that they could be pulled from their array positions for microbiological sampling at various time points.

The MFCs were assembled by placing the anode chambers (holding 50- by 8-mm stirring bars) on top of stirring plates and then positioning the cathode chambers at matching heights using laboratory jacks (Fig. 2). After the Nafion

TABLE 1. Initial and final conditions in the microbial fuel cells[a]

Cell	Whole-cell potential (cathode − anode, V)	Initial pH[b]	Wet wt plankton added (g)	POC (mmol)		Final particulate C/N (mol/mol)	Final DOC (mmol), measured[d]	Final pH[c]
				Initial, calculated	Final, measured[c]			
1	0.4	8.33	36.27	123 ± 1	22.7 ± 1.1	5.4 ± 0.2	3.02 ± 0.07	5.92
2	0.2	7.24	36.25	123 ± 1	24.6 ± 1.2	5.5 ± 0.3	2.79 ± 0.07	6.80
3	0.3	7.24	36.41	124 ± 1	22.7 ± 0.9	5.3 ± 0.2	2.74 ± 0.07	6.99
4	0.4	7.25	36.33	124 ± 1	ND	ND	ND	5.88
5	0.5	7.24	36.72	125 ± 1	21.9 ± 0.5	5.2 ± 0.1	2.88 ± 0.07	6.76
6	0.6	7.26	36.49	124 ± 1	21.7 ± 1.1	5.4 ± 0.1	2.54 ± 0.07	7.55
7	Open circuit	7.26	36.60	125 ± 1	20.4 ± 1.0	5.4 ± 0.1	5.60 ± 0.13	8.46

[a] Reported uncertainties represent standard deviations from means or standard deviations derived by error propagation. ND, not determined.
[b] Measured just prior to plankton additions.
[c] Measured 56.7 days after plankton additions.
[d] Measurement errors in DOC concentrations were assumed to equal 2% of the determined values.

membranes were clamped in place, chamber pairs were secured to a rigid wooden frame and then filled with natural prefiltered (1-μm filter) seawater, drained, refilled, and drained again. The electrode arrays (also prerinsed with filtered seawater) were then introduced, their wires were passed through the reaction heads, and these lids were clamped in place. Above the chambers, all the wires from the removable rods and the fixed portion of each array were soldered together so that all electrode rods served as parallel conductors. Finally, a reference electrode (Ag/AgCl/3mol liter^{-1} KCl) (MI-401F; Microelectrodes, Inc., Bedford, NH) and two 6.4-mm-outer-diameter polyethylene tubes (for the recirculation of cathode seawater; see below) were placed into each cathode chamber. Each anode chamber also contained a combination pH microelectrode (MI-412; Microelectrodes Inc.) and a tube for bubbling with N_2. One anode chamber (cell 4) also was fitted with a temperature probe (TMC6-HD; Onset Computer Corp., Bourne, MA) and an amperometric H_2S microelectrode (H_2S50; Unisense Aarhus, Denmark).

MFC experiments and electrical measurements. The experiments with the seven MFCs took place concurrently in a laboratory maintained at 15 ± 3°C (Fig. 2). Twenty-five days before the introduction of plankton, all cathode and anode chambers (except cell 1) were refilled with 4.5 liters of 1-μm-filtered seawater and monitoring of electrode potentials initiated. Cell 1 was not filled until 6 h before the addition of plankton to it in order to evaluate any effect of unconditioned electrodes. During the experiments, peristaltic pumps circulated oxic seawater past the cathodes (at ~5 liters h^{-1}). Anode volumes were not exchanged but were stirred continuously. Oxygen was purged from the anode chambers initially by bubbling with N_2 gas for 4 h.

Electrical measurements associated with the MFCs were logged with a multimeter (Agilent 34970A data acquisition unit with a 20-channel multiplexer module [34901A]; Agilent Technologies, Palo Alto, CA). Whole-cell potential (cathode − anode), anode potential (anode versus Ag/AgCl/3mol liter^{-1} KCl), and current were recorded generally every 15 min for each cell. Simple passive potentiostats (Northwest Metasystems, Inc., Bainbridge Island, WA) were used for controlling the cell potentials and were connected 16 h after the plankton additions. In this way, current was allowed to pass only after cell potentials were equal to or greater than preset values. Whole-cell potentials were varied between experiments and ranged from 0.2 to 0.6 V (Table 1). Cell 7 was reserved as an open-circuit control.

Plankton and seawater additions. The plankton that was added to the anode chambers was collected by multiple deployments of a 335-μm mesh plankton net in Oregon coastal waters. The net was towed at 2 knots, 1 to 2 m below the sea surface, from the research vessel *Elakha*, approximately 9 km from shore (latitude, +44.65; longitude, −124.18). Captured plankton was washed down into the cod end of the net and then transferred to insulated storage containers. After returning to shore, these samples were separated into size fractions by gentle sieving through nylon screens. The 210- to 1,000-μm fraction was chosen for these experiments. It consisted of a mixture of phytoplankton and zooplankton dominated by diatoms and *Calanus* copepods. After gentle mixing on the surface of the 210-μm screen using a plastic spatula, sample aliquots were divided and weighed. Those prepared for addition to the fuel cells were each approximately 36 g (wet weight) (Table 1) and were transferred to the fuel cells <6 h after collection. Six other splits were separated for determinations of wet/dry weight ratios, ash content, and organic C and N concentrations.

Unused plankton from the 210- to 1,000-μm size fraction that was collected on day 0 of the experiments was stored frozen. During days 44 to 53, five additional

masses of this material, ranging in wet weight from 7 to 20.6 g, were added to cell 4 to test the effect of plankton supplementation on power production. These additions followed breakage and repair (days 38 to 44) of one of the necks entering the anode chamber of cell 4.

The only other additions to the cells occurred 29 days after the initial plankton additions. At this time, 200 ml of sterile, deoxygenated seawater was added to each anode chamber to compensate for liquid removed in chemical sampling. These seawater aliquots were prepared by autoclaving 1-μm-filtered seawater for 60 min and then bubbling 500-ml volumes with N_2. The N_2 was first passed through a HEPA vent filter and dispersed with a sterile glass dispersion tube. During these additions, each anode array was also agitated up and down gently to dislodge particulate material trapped within the array. (As discussed below, this was only partially successful.)

Chemical sampling and analyses. Time courses of chemical changes were determined by semicontinuous microelectrode measurements and by the withdrawal and analysis of discrete samples from each anode chamber. The potentials of the pH microelectrodes were recorded after amplification, with the Agilent multimeter used for logging the MFC electrical parameters. These potentials were converted to pH according to the results of calibrations repeated regularly with National Bureau of Standards (NBS) buffers at 15°C. H_2S and temperature sensor measurements (cell 4 only) were logged with independent instrumentation: a Unisense PA2000 picoammeter interfaced with a voltage logger (VC4-300; MicroDaq, NH) and a HOBO U12-012 temperature logger (Onset Computer Corp., Bourne, MA). The H_2S sensor current (pA) was calibrated as a function of H_2S concentration in an anoxic 2-aminopyridine solution buffered at pH 7.0 to which standard additions of Na_2S stock solution were made. The presence of the buffer limited the increase in pH to <0.1 during sulfide additions. Therefore, the H_2S concentration could be readily calculated from the total sulfide concentration, the pH (NBS scale), and the first dissociation constant for hydrogen sulfide (K'_1) (22, 34). The electrode-based determinations of total sulfide concentration in the anode chamber of cell 4 depended on similar calculations using equilibrium relationships and sensor measurements of pH and H_2S.

Sampling of each chamber began at specified times ~5.2 days before the plankton additions, included time points <0.5 h after the additions, and continued biweekly over 56.7 days. During flushing of the chamber headspace, approximately 6 ml of "anode water" was withdrawn through a Teflon needle into a gas-tight syringe, and the syringe was transferred into a glove bag containing an N_2 atmosphere. Each sample volume was then filtered through a 0.45-μm Supor syringe filter (Gelman), and three 1 ml aliquots were taken and fixed with 0.1 ml of diamine reagent for determinations of total dissolved sulfide (8). The remaining volume was separated into aliquots for later analyses of nutrients [NO_3^-, NO_2^-, NH_4^+, PO_4^{3-}, and $Si(OH)_4$], metals (Mn and Fe), and major ions (SO_4^{2-} and Cl^-). Standard autoanalyzer (Alpkem, Clackamas, OR), ICP-optical emission spectrometer (Teledyne-Leeman, Hudson, NH), and ion chromatograph (Dionex, Sunnydale, CA) methods were employed for these determinations, respectively.

A second set of time series samples were withdrawn for suspended POC and total nitrogen (POC/N), DOC, and dissolved inorganic carbon (DIC) determinations. For these samples, all glass vials (2 drams), caps (lined with Teflon/silicon septa), and filtering glassware were prewashed in 10%HCl and thoroughly rinsed in deionized water (Millipore, 18.2 MΩ cm^{-1}). Vials, glassware, filters, Al foil, and forceps were also heated to and held at 500°C for 4 h before use. Using

a pipettor with a wide-bore tip, three 5-ml aliquots of anode water were removed and each filtered through separate 25-mm GF/F filters with a glass vacuum filtering apparatus with a 15-ml funnel and hand vacuum pump. The GF/F filters were then individually folded with forceps, wrapped in Al foil, and frozen for later POC/N analyses. From the 15 ml of combined filtrate, triplicate 4-ml samples for DOC analyses were withdrawn and transferred to vials containing 50 μl concentrated phosphoric acid. The remaining filtrate was preserved for DIC analyses in vials by mixing with 12 μl saturated $HgCl_2$.

DIC concentrations were measured after CO_2 evolution using a 1.5-ml sample loop, phosphoric acid addition, and a CO_2 coulometer (UIC Inc., Coulometrics, Joliet, IL). DOC was analyzed by high-temperature oxidation with a Pt catalyst, utilizing a Shimadzu TOC-V analyzer. Filters retaining POC/N as well as bulk plankton samples were dried, decalcified by exposure to acid fumes, and analyzed for their OC and total nitrogen contents with a Carlo Erba NA-1500 CN analyzer.

It was observed from the very start that some particulate matter from the plankton did not stay in suspension but instead settled out and became trapped around the anode arrays, where it was not readily subsampled. Therefore, to quantify the final amount of POC/N remaining at the end of each experiment, anode chamber lids were removed and the anode arrays agitated up and down vigorously to dislodge adhering particulate matter. Fifteen 10-ml samples were then withdrawn and filtered, and the filters were treated and analyzed using the same methods applied to the time course samples. The remaining volume of anode water was measured with a graduated cylinder, and this volume was also calculated based on previously specified sample withdrawals and seawater additions (with good agreement). The average concentration of POC/N per ml ($n = 15$) multiplied by the volume before the removal of final samples is reported as final POC or N. Reported uncertainties represent standard deviations from means or standard deviations derived by propagation of errors.

Microbial community sampling and analyses. Biological sampling accompanied five of the chemical sampling times. Pairs of graphite- and glassy carbon-impregnated rods were removed with flame-sterilized forceps from both anode and cathode chambers. The wires to these rods were cut, and the rods were cut into thirds with a Dremel tool blade that had been sterilized with alcohol and a propane flame. One-third of each rod was scraped with an alcohol-flame-sterilized razor blade. These scrapings were preserved in a filter-sterilized 1:1 solution of ethanol and isosmotic phosphate-buffered saline and then frozen at −50°C. In this report, only the results of DNA extractions from graphite scrapings at the final sampling times of cells 3, 6, and 7 are presented.

Nucleic acids were extracted with the PowerSoil DNA extraction kit (MoBio Inc., San Diego, CA), modified to maximize yields (16). Small-subunit (SSU) rRNA bacterial genes from all samples were amplified by PCR (42) with a bacterial targeted forward primer (B27f, 59-AGAGTTTGATCCTGGCTCAG-39) and a universal reverse primer (U1492r, 59-GGTTACCTTGTTACGACTT-39). Environmental rRNA clone libraries were constructed by cloning amplicons into a pCR4 TOPO vector and transforming into chemically competent *Escherichia coli* according to the manufacturer's protocol (TOPO TA cloning kit; Invitrogen Inc.). Transformants were screened on LB–kanamycin–X-Gal (5-bromo-4-chloro-3-indolyl-β-D-galactopyranoside) plates using blue-white selection. Plasmids were purified with the Montage miniprep kit (Millipore, Inc.) and sequenced with BigDye chemistry (version 3.1) on an ABI 3730 capillary sequencer. Ninety-six plasmids were sequenced and compared in both directions from each anode sample. SSU rRNA sequences were trimmed of vector using Sequencher 4.0 (Gene Codes Inc., Ann Arbor, MI). SSU rRNA sequence data were compiled and aligned to full-length sequences obtained from GenBank with the FASTALIGNER alignment utility of the ARB program package (www.arb-home.de). Alignments were verified by comparison of the sequences of secondary structure with those of *Escherichia coli* and closely related phylotypes. Phylogenetic analysis of the bacterial SSU rRNA sequences was accomplished with MrBayes version 3.1.2. The evolutionary model was set to the general time-reversible model, with rates equal to the inverse of gamma. Six hundred thousand generations were run, with sampling every 100 generations, and burn-in was set to 6,000.

Nucleotide sequence accession numbers. The 16S rRNA sequences of the rRNA clones described in this study have been deposited in GenBank under accession numbers EU052237 to EU052266.

RESULTS

Plankton decomposition and chemical behavior of the MFCs. The plankton added to the MFCs had an initial dry-to-wet weight ratio of 0.114 ± 0.001 ($n = 6$) and an ash content of 26.2% ± 0.2% ($n = 3$). Its OC content was 35.9% ± 0.3% and total nitrogen 8.7% ± 0.1% (dry weight) ($n = 3$). From these analyses, the initial amounts of POC added in the seven experiments were assessed (Table 1), as were the initial POC concentrations (27.5 ± 0.1 mmol liter^{-1}) and C/N atomic ratios (4.82 ± 0.03).

The most immediate chemical change after the plankton additions was a rapid decline in suspended POC (and N), accompanied by a release of DOC, dissolved phosphate, and ammonium (Fig. 3). This evolution was followed over the first 2 weeks by rising levels of total sulfide, DIC, and silicic acid; a moderate decline in sulfate (Fig. 4); and the onset of MFC current production in cells 1 to 6 (Fig. 5 and 6). Further plankton additions to cell 4 showed that peak currents could be renewed and increased (Fig. 6). The cells with the highest cell currents (cells 1 and 4; both at 0.4 V) also exhibited the greatest decline in pH, which affected measured silicic acid levels and DIC (Table 1; Fig. 4). These changes were presumably due to shifts in chemical speciation and associated losses by polymerization of $Si(OH)_4$ and CO_2 degassing.

All experiments with single plankton additions and active electrodes became depleted of dissolved sulfide and showed greater DOC consumption than the open-circuit control in later weeks (Fig. 3 and 4). Seawater additions (4% by volume) and agitation of the anodes on day 29 offset some chemical trends and had a large effect on the suspended POC/N ratio (Fig. 7). However, final POC/N ratios and amounts (determined after vigorous shaking and removal of the anodes) were effectively the same in every single-addition experiment (Table 1). These final determinations compared to those prior to the breakdown of the experiments (see Materials and Methods) also indicate that on average 15 mmol POC (representing a concentration of 3.5 mmol liter^{-1}) either was trapped by or adhered to the anode arrays (Fig. 3A).

To test whether there were significant differences between means in the final amounts of DOC, POC, and total OC (TOC) (DOC + POC) in active fuel cells ($n = 5$) versus the final amounts in the open-circuit control, two-tailed Student t tests (52) were applied after grouping the data in Table 1. These tests confirmed that only DOC was significantly different in comparison to the control ($P < 0.001$ for DOC, $0.2 < P < 0.5$ for POC, and $P > 0.5$ for TOC). The percentage of the initial OC added as plankton but remaining in these residual OC pools is reported in Table 2. Final DIC accumulations are not tabulated but were equal to only 1 to 68% of corresponding TOC losses due to the variable amounts of CO_2 degassing from the cells (cell 1 exhibited the greatest and cell 7 the least [Fig. 4D]).

Comparative performance of the MFCs and anode microbial communities. Electrode potentials during the MFC experiments are illustrated in Fig. 8. Because the concentrations of electroactive species (dominantly HS$^-$) in the anode chamber rose and fell in a broad pulse rather than remaining at relatively constant values for a period of time, widely used models of current-voltage behavior based on quasi-steady-state bulk concentrations are not appropriate here for characterizing performance. However a qualitative description of current-potential behavior is possible.

In general, the current and voltage behavior of each active cell can be divided into two domains based on the concentra-
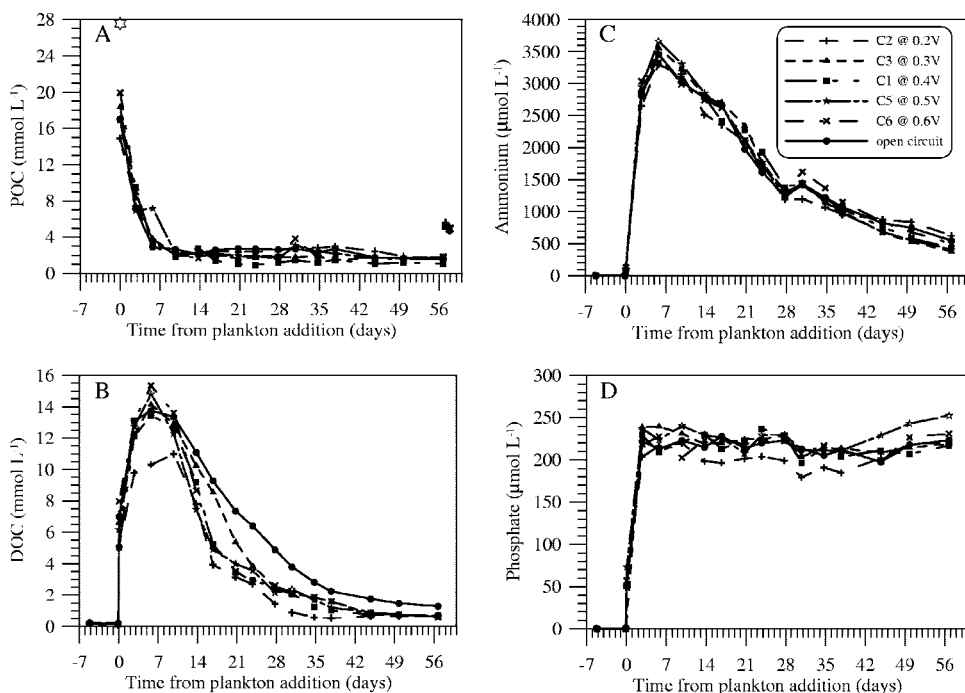
FIG. 3. Time courses of POC (A), DOC (B), ammonium (C), and phosphate (D) in cells 1 to 3 and 5 to 7. The identification of symbols and lines is the same in all panels. In panel A the star at day 0 corresponds to initial POC concentrations computed from the weight of plankton added, its dry/wet weight ratio, and the OC content of dry material. Final data points in panel A were measured after vigorous resuspension of all particulate materials adhered to the anode arrays. These points are on average 3.5 mmol liter^{-1} greater than the prior time points before resuspension.

tion of electroactive species in the anode chamber, with the concentration of O_2 in the cathode chamber being approximately constant. From day 7 to ~25 (or 32 for cell 3), when concentrations of electroactive species in the anode chamber

were high, the resulting high current caused modest polarization of the cathode as indicated by the drop in cathode potential. During this period, polarization of the anode is difficult to characterize because the anode potential was responding to
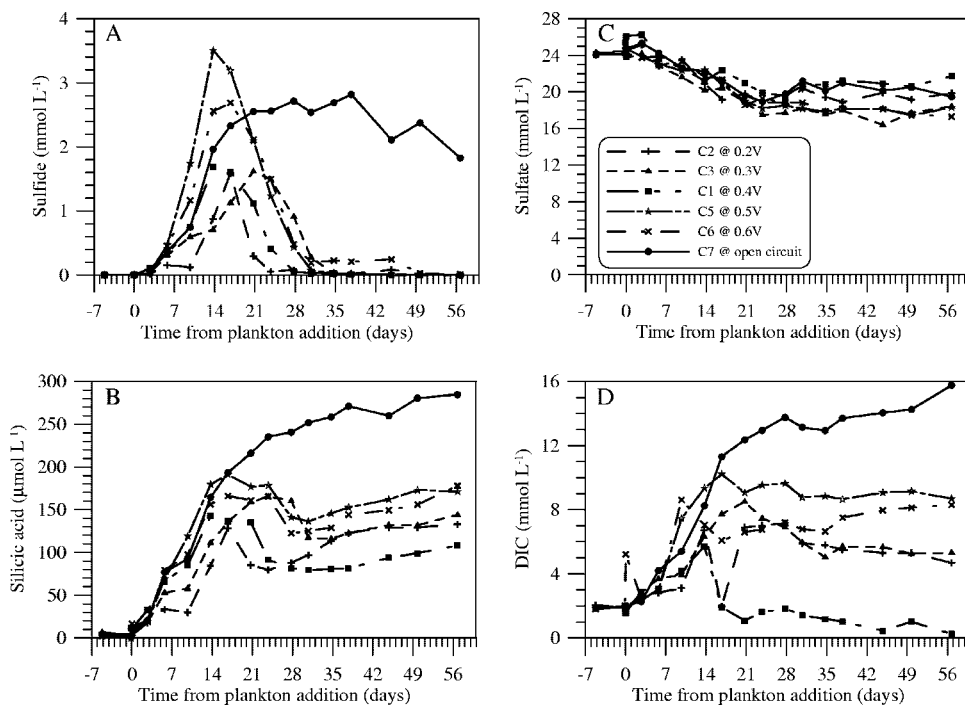

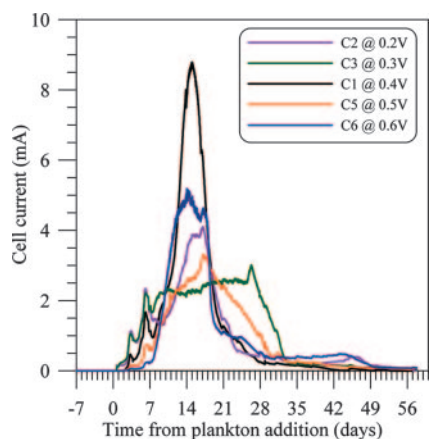FIG. 4. Time courses of total sulfide (A), silicic acid (B), sulfate (C), and DIC (D) in cells 1 to 3 and 5 to 7.

FIG. 5. Time courses of current production by cells 1 to 3, 5, and 6.

FIG. 7. Ratios of POC to total nitrogen in subsamples collected on filters throughout the experiments. The symbols have the same meanings as in Fig. 2.

the changes in both concentrations and current. However the anode potential was still more positive than that in the control cell 7. From day ~26 through 56.7, the cathode was well poised with relatively high concentrations of O_2 at approximately +0.34 to +0.40 V versus AgCl/Cl, and the anode, with very low concentrations of electroactive species, was polarized at potentials that reflect the various whole-cell voltages. The reference electrode was in the cathode chamber, so anode polarization includes any polarization at the membrane separating the two chambers. Also, we note that because the electrodes of cell 1
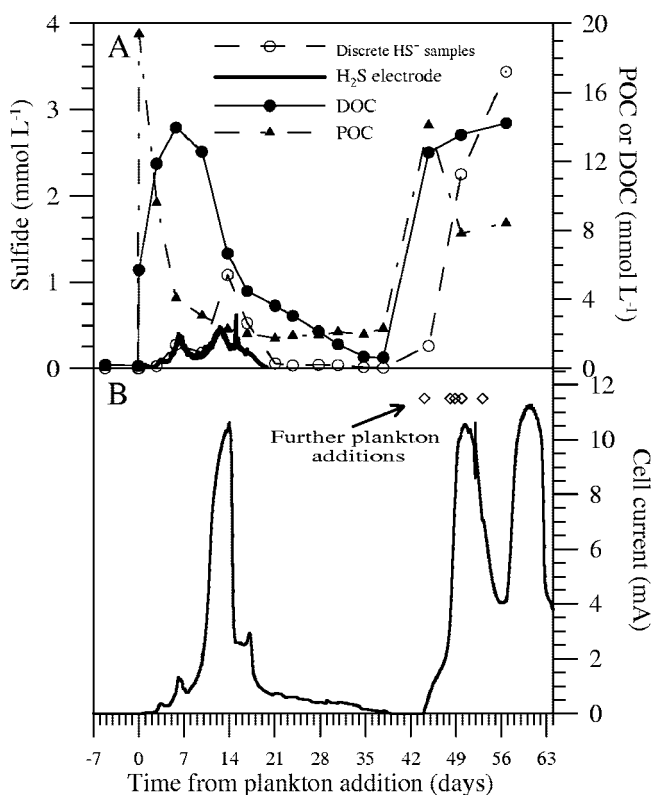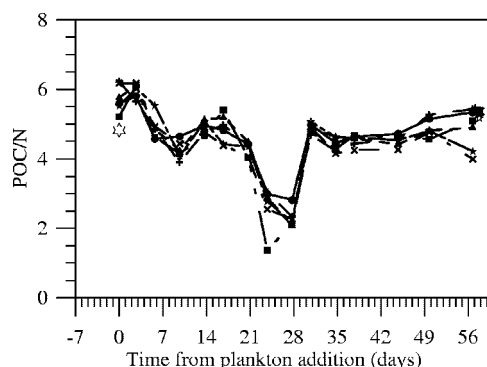

FIG. 6. Subset of the chemical data (A) and current associated with cell 4 (B). The times when further plankton additions were made in this experiment are indicated by the diamonds in panel B.

were not preconditioned in seawater, both the anode and cathode potentials of this cell lagged those of its counterparts by approximately 3.3 days.

Separate evidence that the cathode surface area had an overall limiting effect on the current (and thus power density) when concentrations of electroactive species were high in the anode chamber was found by additional manipulations of cell 4. On day 51 (when a current spike appears in Fig. 6), electrode rods were disconnected and reconnected (by wire cutting and resoldering) from both sides of the circuit to create nine different ratios of cathode to anode area, ranging from 0.034 to 29. The current was then monitored over time intervals of approximately 15 min per ratio. The resulting average power density (if calculated per area of anode) increased with increasing cathode/anode ratio and varied from 1.6 to 289 mW m^{-2}. At a 1:1 ratio, the power density was 15 mW m^{-2} during these manipulations (data not shown).

The effective electrical resistances of the cells were determined simply by dividing the whole-cell potentials by the currents (data not shown). The minimum in this resistance was approximately 38 Ω, which occurred at the current peaks of cell 4. Because the medium was seawater, the ohmic resistance of the solution was not significant in these cells. However, the ohmic resistance of the Nafion membrane plus possible contact resistances within the circuit may be assumed to have approached the minimum resistance.

MFC reactions produced between 4,356 and 5,846 C per single-batch experiment. These yields equate to current efficiencies of 11.3 to 15.5% if all the OC consumed (or otherwise not accounted for in residual fractions) is assumed a source of 4 electrons per C atom (Table 2). Because cell 3 had a broad and prolonged current maximum (Fig. 5), the highest efficiencies did not necessarily correspond to the cells with the highest currents or power densities. The MFC discharged at the highest voltage (cell 6) yielded the greatest overall energy (Table 2).

The relatively stable anode potentials over the last 30 days of the experiments provided an opportunity to determine if the microbial communities recovered from each anode varied as a function of anode potential. Figure 9 compares the representative phylotypes found to be associated with anodes from cells 3, 6, and 7 on day 56. These were allied with *Epsilon-*, *Delta-*,

TABLE 2. Comparison of the performances of microbial fuel cells[a]

Cell	Maximum power density (mW m^{-2})	Residual POC (% initial POC)	Residual DOC (% initial POC)	Coulombs produced	Energy produced (kJ)	Current efficiency (% POC consumed) [% POC added]
1	12.5	18.4 ± 0.9	2.44 ± 0.06	5,846	2.34	15.5 [12.3]
2	2.9	19.9 ± 1.0	2.26 ± 0.06	4,570	0.91	11.8 [9.6]
3	3.2	18.3 ± 0.7	2.21 ± 0.06	5,647	1.69	14.6 [11.8]
4	14.9[b], 17.2[c]	ND	ND	5,151[b]	2.07[b]	13.6 [10.8][b]
5	5.9	17.5 ± 0.4	2.30 ± 0.06	4,356	2.17	11.3 [9.0]
6	11.0	17.5 ± 0.9	2.05 ± 0.05	4,994	3.00	13.0 [10.4]
7		16.4 ± 0.8	4.49 ± 0.11			

[a] Reported uncertainties represent standard deviations from means or standard deviations derived by error propagation. ND, not determined.
[b] From 0 to 39 days and before secondary plankton additions.
[c] After secondary plankton additions.

and *Gammaproteobacteria* as well as the *Flavobacterium-Cytophaga-Bacteroides* and *Fusobacteria* groups. Library representation, which is only a qualitative assessment of abundance, is summarized in Table 3. There are few differences between the phylotypes identified in these samples. Most notably, the *Delta-* and *Gammaproteobacteria* are similarly represented in the open-circuit library compared to those held at potential. Ribotypes allied with the *Flavobacterium-Cytophaga-Bacteroides* and *Epsilonproteobacteria* show qualitative differences between cells, but these changes are not in the order of anode potential. Only ribotypes allied with the *Fusobacteria* are uniquely represented in clones from the open-circuit cell 7 (Table 3).

DISCUSSION

Marine particulate organic matter decomposition under anoxic conditions has been shown to begin with exoenzymatic hydrolysis of macromolecular organic matter to form dissolved organic matter, followed by fermentation and respiration of volatile fatty acids by prokaryotic organisms (6, 19, 23). Fresh plankton has also been demonstrated to release extremely bioreactive dissolved organic matter by cell lysis (36) and to result in decomposition rates that vary among classes of biochemical compounds (17). Kinetic models used to describe these organic matter decomposition processes typically assume that terminal respiration steps are rate limiting and incorporate multiple fractions of organic materials with different reactivities.

To illustrate one fairly simple model for describing the degradation of plankton, we present the expression:

$$G_T(t) = G_1 \exp(-k_1 t) + G_2 \exp(-k_2 t) + G_{NR} \qquad (1)$$

which was applied by Westrich and Berner (49) to simulate decomposition of TOC. In this expression G_T represents the concentration of TOC, there are two major decomposable fractions (G_1 and G_2) that are assumed to undergo decomposition via first-order kinetics, and there is a nonreactive fraction (G_{NR}). By incubating plankton under oxic conditions, Westrich and Berner (49) observed the relative proportions of G_1 to G_2 to G_{NR} to be 50:16:34. Similar studies using pure phytoplankton cultures have shown that overall rates of POC decay under oxic conditions were 4 to 6 times greater than those under anoxic conditions and that oxic conditions resulted in nearly complete carbon degradation (15, 17). These results are frequently interpreted to suggest that oxygen serves not only as the most energetically favorable respiratory electron
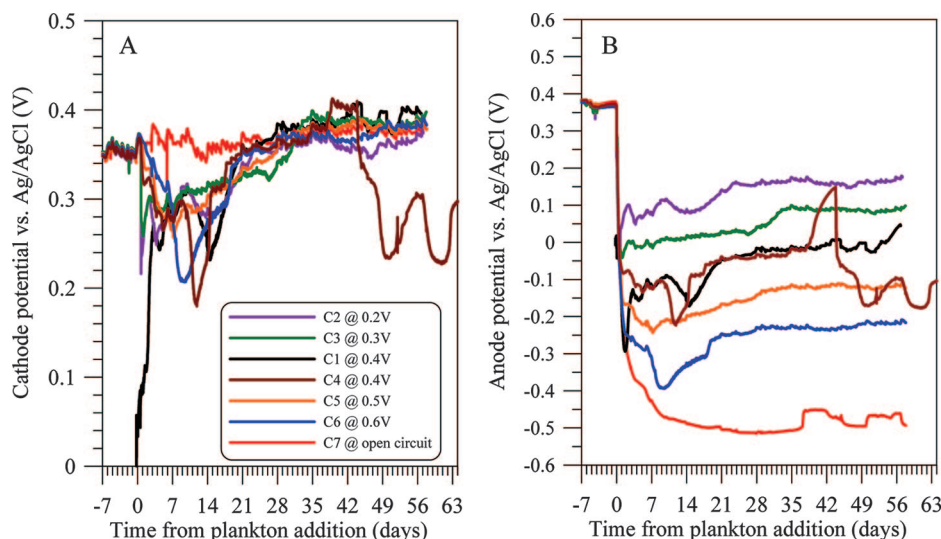

FIG. 8. Time courses of cathode (A) and anode (B) potentials versus Ag/AgCl (3 M KCl) from cells 1 to 7. Oxygen entered the anode chamber of cell 4 during days 38 to 44 due to breakage of the chamber lid.
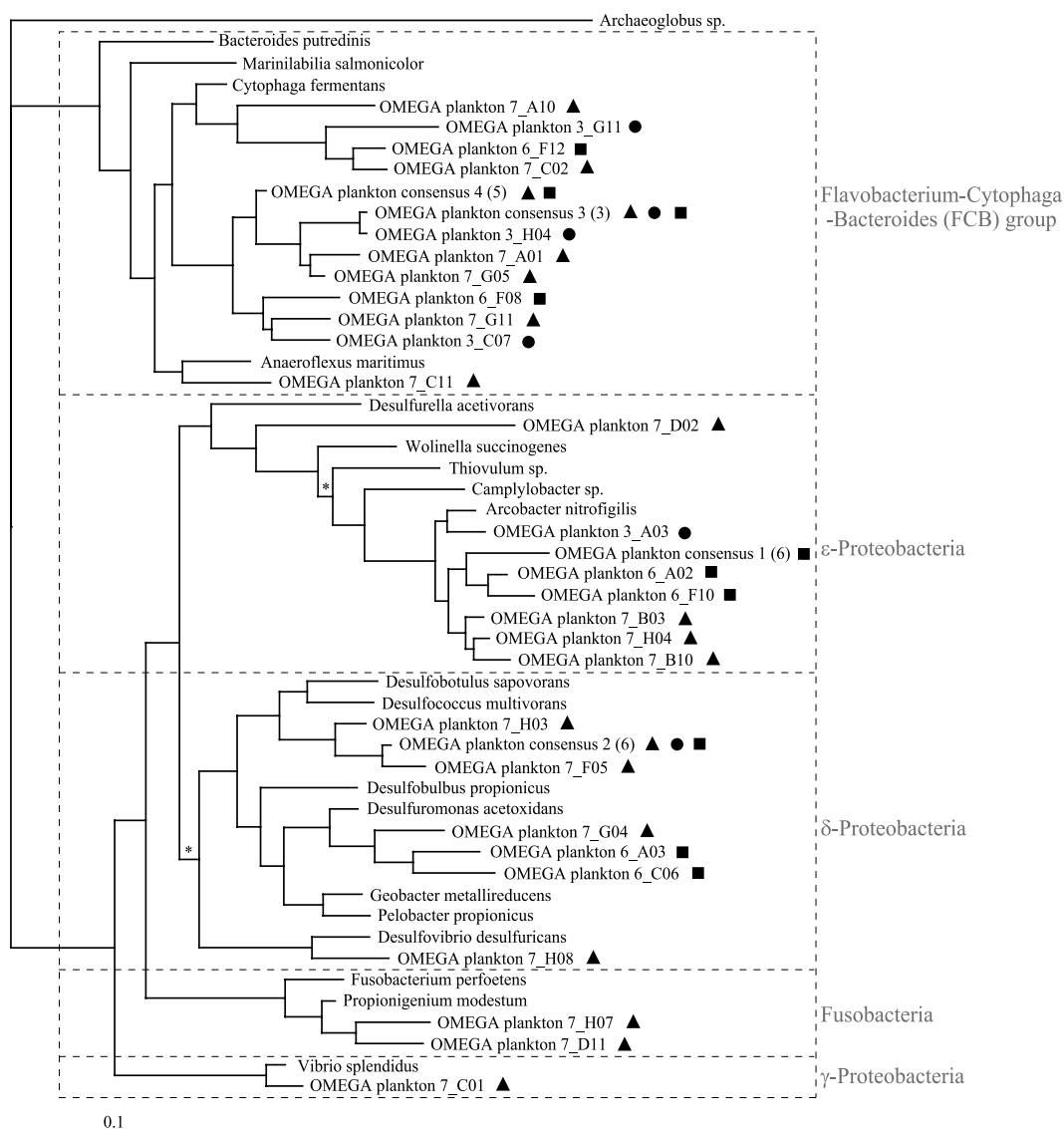
FIG. 9. Phylogenetic tree constructed by Bayesian analysis, showing dominant phylotypes from anodes of plankton-fed MFCs. Trees constructed with other reconstruction algorithms (distance, parsimony, and maximum likelihood) resulted in the same overall topology. *Archaeoglobus* sp., an archaean, was used as the outgroup. Symbols denote sequences recovered from individual fuel cells held at 0.3 V (dots), 0.6 V (squares), and open circuit (triangles). Consensus sequences are indicated, and the number of individual sequences contributing is shown in parentheses. In some instances consensus sequences are followed by more than one symbol, indicating that the sequences from which they are composed were recovered from more than one fuel cell. Posterior probabilities were 1 except as indicated by the asterisk (0.5).

acceptor but possibly as a cofactor for microbial enzymes such as oxygenases that are able to depolymerize refractory organic materials (7).

The results of the plankton incubation within the control MFC (cell 7) conform to the decomposition representation described above. The TOC at each sampling time was computed as the sum of measured DOC, POC, and the POC that was found to be trapped around the anode arrays (3.5 mmol liter^{-1} [Fig. 3A]) (Fig. 10). The model in equation 1 was then fitted to these data with Grapher scientific graphing software (Golden Software, Inc). The model indicates that 7.5% of the TOC in cell 7 was highly bioreactive ($k_1 = 0.79$ day^{-1}), 81.9% degraded more slowly ($k_2 = 0.037$ day^{-1}), and 10.6% of the carbon was refractory ($r^2 = 0.993$). As extracted dissolved

organic matter and cell debris from a culture of marine diatom cells have been found to have decay rates of 1.2 to 1.7 day^{-1} and 0.047 to 0.055 day^{-1}, respectively, at 20°C in the presence of oxygen (36), we suspect that two similar organic fractions contributed to the reactive materials in this study (15°C, anoxic, mixed plankton source).

Other measurements of chemical changes within cell 7 indicate that the TOC loss was coupled tightly to sulfate reduction. For example, dissolved nitrate plus nitrite, manganese, and iron concentrations were at all times less than 4, 2, and 0.1 μmol liter^{-1}, respectively (data not shown), which signifies the trace availability of alternate electron acceptors. Sulfate concentrations (which replicate measurements showed were not very precise) declined by ~5 mmol liter^{-1} over the first 28 days

TABLE 3. Proportions of major phylogenic groups of bacteria found in clone libraries from anode samples

Bacterial group	Most closely related species	% in cell:		
		3	6	7 (open-circuit control)
Flavobacterium-Cytophaga-Bacteroides	*Cytophaga fermentans, Anaeroflexus maritimus*	52	20	53
Epsilonproteobacteria	*Arcobacter nitofigilis*	6	54	20
Deltaproteobacteria	*Desulfobotulus sapovorans, Desulfuromonas acetoxidans, Desulfovibrio desulfuricans*	33	25	23
Gammaproteobacteria	*Vibrio splendidus*	9	1	3
Fusobacteria	*Propionigenium modestum*	–	–	1

of the experiment, and sulfide concentrations rose through day 37 (Fig. 4). A plot of TOC versus sulfate that is restricted to days 0 to 28 yields a slope of 2.0, the ideal stoichiometry for oxidation of OC to CO_2 and reduction of sulfate to sulfide (Table 4, cell 7). On day 29, seawater additions elevated sulfate concentrations, with a small decline in sulfate continuing subsequently in cell 7. It is also possible that some sulfide was reoxidized to sulfate or other sulfur species with an intermediate oxidation state(s) throughout the experiment due to oxygen diffusion into the anode chamber through the Nafion membrane (26). Methanogenesis and sulfate reduction coupled to methane oxidation are assumed to have been insignificant, because heterotrophic sulfate-reducing bacteria are known to dominate metabolic processes under anoxic conditions replete in sulfate (23, 46, 50). Sequences from sulfate-reducing bacteria also comprised a major proportion of the SSU clone library generated from the anode scrapings (Table 3; Fig. 9).

In contrast to cell 7, all other cells exhibited a departure from normal anoxic plankton decomposition models as indicated by the TOC time courses. Figure 10 illustrates this change using data from cells 1 and 3 (with cell 3 exhibiting the least pronounced of all changes). During the third week of the active MFC experiments, the rate of TOC consumption increased. This carbon loss can be attributed to a significant decrease in DOC, with offsets from cell 7 being greatest shortly after peak currents in most cells. The implication is that once microbial communities became established on the active fuel

cell anodes, respiration coupled either directly or indirectly to electricity generation was enhanced until the metabolizable fraction of the DOC pool was nearly exhausted. This occurrence did not significantly alter the final TOC concentration, but it did significantly reduce DOC levels (with corresponding increases in the slopes of most TOC/SO_4^{2-} mol/mol plots) (Table 4).

To address what process(es) could have linked carbon degradation to electricity generation, we will first review the current efficiencies of these MFCs. The current efficiencies were 11.3 to 15.5% (Table 2), with 85 to 97% of each cell's cumulative electron flux occurring within the first 28 days after the plankton additions. If these efficiencies were computed relative to the TOC added instead of the TOC consumed, they would decline to 9.0 to 12.3% (Table 2). Thus, as has been observed in MFCs supplied with high concentrations of complex organic wastes, a large portion of the fuel was oxidized without passing electrons to the electrodes (18, 27, 35).

It is evident from this study and others that there can be multiple anodic reactions in seawater-based MFCs and that certain reactions do not result in high current efficiencies (12, 45). As introduced earlier, electrons can be transferred "directly" from organic substrates by microorganisms that utilize an active fuel cell anode as an electron acceptor [in the same way that some microorganisms can use insoluble Mn(IV) or Fe(III) oxides to accept electrons during respiration]. Alternatively, electrons can be derived indirectly from organic matter by the abiotic anodic oxidation of microbially generated sulfide (Fig. 11). A dominance of organic matter oxidation by "anodophilic" organisms that directly shuttle electrons to a fuel cell electrode is expected to result in a high current efficiency, generation of acid, and a stoichiometric ratio of ΔTOC to ΔSO_4^{2-} of $\geqslant 2$. Analogous to iron reduction in sediments (32, 44), this process may have the capacity to outcompete organic
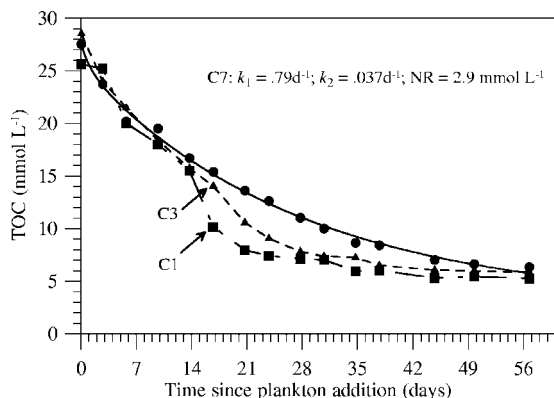

FIG. 10. Time courses of TOC from cells 7, 1, and 3. Data from cell 7 were fit to a multicomponent decomposition model from which decay constants (k_1 and k_2, day^{-1}) and a nonreactive fraction (NR) were derived.

TABLE 4. Slopes of TOC-versus-sulfate plots during the first 28 days of the time courses[a]

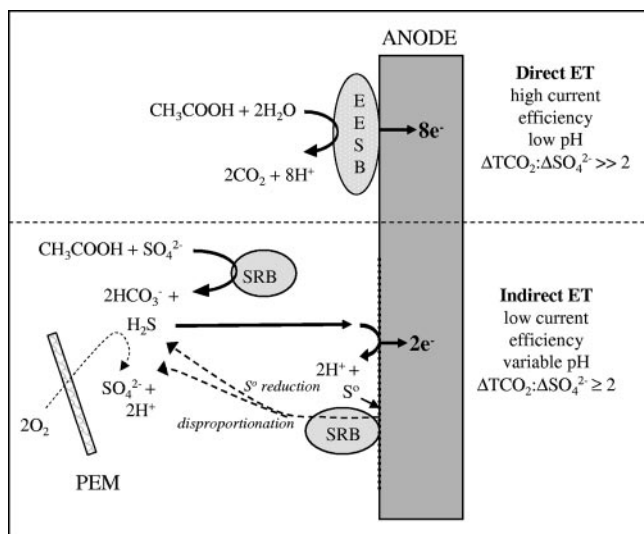| Cell	TOC/SO_4^{2-} (mol/mol)	r^2
1	2.6	0.89
2	2.1	0.95
3	2.6	0.95
4	3.7	0.97
5	2.7	0.85
6	3.2	0.86
7	2.0	0.89

[a] $n = 9$ for all regressions.

FIG. 11. Schematic of competing anode reactions in a seawater-based MFC. EESB, exocellular electron-shuttling bacterium; SRB, sulfate (or S^0)-reducing bacterium; PEM, proton exchange membrane. The extent of sulfide reoxidation to sulfate determines the pH and $\Delta TOC/\Delta SO_4^{2-}$ observed when electron transport is indirectly from organic matter.

matter oxidation coupled to sulfate reduction and to consume dissolved organic matter at a higher rate in plankton MFCs (although a quantitative prediction of a rate for such a heterogeneous, microbially mediated reaction is quite difficult). In addition, organic matter oxidation directly coupled to an electrode may act like direct oxygen exposure to stimulate microorganisms (such as those in the *Flavobacterium-Cytophagales-Bacteroides* group, which produce extracellular enzymes) to depolymerize high-molecular-weight organic compounds. Thus, one interpretation of the accelerated consumption of DOC that started within the third week of the active MFC time courses is that it is evidence for direct organic matter oxidation mediated by microbial communities attached to the anodes. This explanation is most consistent with the behavior of cells 1 and 4, which exhibited the highest current peaks and lowest final pH values.

An alternative interpretation is that the higher rate occurred as a consequence of the removal of sulfide from the anode solutions by electrochemical oxidation at the anode. If high sulfide concentrations have an inhibitory effect on sulfate reducers, as has been suggested by McCartney and Oleskiewicz (33) and Roychoudhury et al. (44), then electrochemical removal of sulfide could have stimulated the activity of sulfate-reducing bacteria either within anode biofilms or within the surrounding solution. Furthermore, if electrochemical sulfide oxidation resulted primarily in the formation of species such as polysulfides or elemental sulfur (which has been confirmed repeatedly [see 45 and references therein]), this process alone could explain current efficiencies of ≤25%. Surprisingly however, many of the active MFCs did not maintain consistent $\Delta TOC/\Delta SO_4^{2-}$ relationships during the period of accelerated TOC loss, as indicated in Table 4. The only way to reconcile all the solution data is to invoke a substantial production of sulfate because of sulfide reaction with oxygen that diffused across

the proton exchange membrane (27) and/or to assume that heterotrophic bacteria associated with the anode biofilm accelerated TOC decomposition primarily by rereducing (or disproportionating) elemental sulfur (instead of sulfate). It has been demonstrated recently that bacteria that are nominally sulfate-reducing bacteria are also able to reduce elemental sulfur or thiosulfate or to use these sulfur compounds for disproportionation reactions during anaerobic metabolism (24). As is illustrated in Fig. 11, any or all of these sulfur reactions could have intercepted the flow of electrons from organic matter to the fuel cell and altered the $\Delta TOC/\Delta SO_4^{2-}$ stoichiometry. We favor the role of elemental sulfur on the anode as an electron acceptor for sulfate-reducing bacteria because this is a response consistent with the electroactivity of sulfide, the delayed timing of accelerated TOC degradation, and the relatively high proportion of sulfate- and sulfur-reducing *Deltaproteobacteria* in the phylogenetic surveys. In particular, phylotypes related to *Desulfuromonas acetoxidans* can be expected to have the ability to reduce elemental sulfur while oxidizing dissolved organic acids (37).

Furthermore, because there were no preestablished anode communities of bacteria capable of exocellular electron transfer at the start of these single-batch experiments, the MFCs were not primed to directly respond to the most bioreactive organic matter released by cell lysis. The exception was cell 4, which did show an increase in power production in rapid response to supplemental plankton additions. The microbial phylogenetic surveys reveal that a diverse assemblage of phylotypes had colonized the anodes by the end of the experiments. While such surveys are not strictly quantitative, there were some shifts in library representation between the three cells analyzed (Table 3). In particular, we observed a large decrease in the library representation of *Flavobacterium-Cytophagales-Bacteroides* phylotypes on the active anode of cell 6, concomitant with a large increase in the library representation of *Epsilonproteobacteria*. *Cytophagales*-like phylotypes have been found to be metabolically active in anoxic Wadden Sea sediments and to be associated with water column aggregates of particulate organic matter (29). Many of these are specialized in the degradation of complex organic macromolecules (9, 23), and they have been identified repeatedly as members of biofilms on sediment MFCs (20, 42) together with members of the *Deltaproteobacteria*, which are known anode colonizers (4). The dominance of *Epsilonproteobacteria*, however, is a new observation in MFCs. *Epsilonproteobacteria*, in particular those allied to the genus *Arcobacter*, have been found associated with water column particulate organic matter (10), have been associated with bacterial utilization of low-molecular-weight dissolved organics (9), and include strains that are sulfide oxidizers (51). We posit from this that the *Epsilonproteobacteria* were better poised to take advantage of the anode (or covariables such as anodic by-products or associations with other anodic phylotypes) under the conditions of cell 6. Furthermore, an analysis of population shifts during the time courses using terminal restriction fragment length polymorphism analysis (28) and quantitative PCR is currently under way. These analyses may indicate changes in microbial phylotype diversity and density that are not evident in the community composition surveys from the end point samples. An area of exciting future work would be to determine the temporal changes in microbial

biofilm diversity and density in new multiple-batch or pulsed plankton addition fuel cell experiments.

Conclusions. In this study, marine plankton was observed to be an effective energy source in an MFC. In seven experiments roughly 80% of the OC added as fresh substrate was degraded. Current efficiencies were only 11.3 to 15.5%, but this can be attributed to losses through the two-chamber-MFC, single-batch design of these exploratory experiments and competition with the sulfur cycle. Current efficiencies also did not depend strongly on the discharge potential, but because anodic processes were generally limiting, discharge potential tended to regulate anode potential. It is promising that sulfur-reducing microorganisms appeared to accelerate organic matter degradation rates midway through these experiments. If some of this acceleration was directly coupled to the anode by exocellular electron transfer, it suggests that preinoculated, pulse-fed MFCs (perhaps of the upflow type [18, 40]) could be optimized to generate electricity from plankton at a significantly higher efficiency. Plankton decay time courses were also consistent with our understanding of organic matter degradation under anaerobic conditions, sulfide inhibition, and competition between microbial redox processes.

REFERENCES

1. **Aller, R. C.** 1994. The sedimentary Mn cycle in Long Island Sound: its role as intermediate oxidant and the influence of bioturbation, O_2, and C_{org} flux on diagenetic reaction balances. J. Mar. Res. **52:**259–295.
2. **Andersen, L. A., and J. L. Sarmiento.** 1994. Redfield ratios of remineralization determined by nutrient data analysis. Glob. Biogeochem. Cycles **8:**65–80.
3. **Bard, A. J., and L. R. Faulkner.** 2001. Electrochemical methods fundamentals and applications, 2nd ed. John Wiley and Sons, New York, NY.
4. **Bond, D. R., D. E. Holmes, L. M. Tender, and D. R. Lovley.** 2002. Electrode-reducing microorganisms that harvest energy from marine sediments. Science **295:**483–485.
5. **Bond, D. R., and D. R. Lovley.** 2003. Electricity production by *Geobacter sulfurreducens* attached to electrodes. Appl. Env. Microbiol. **69:**1548–1555.
6. **Brüchert, V., and C. Arnosti.** 2003. Anaerobic carbon transformation: experimental studies with flow-through cells. Mar. Chem. **80:**171–183.
7. **Burdige, D. J.** 2007. Preservation of organic matter in marine sediments: controls, mechanisms, and an imbalance in sediment organic carbon budgets? Chem. Rev. **107:**467–485.
8. **Cline, J. D.** 1969. Spectrophotometric determination of hydrogen sulfide in natural waters. Limnol. Oceanogr. **14:**454–458.
9. **Covert, J. S., and M. A. Moran.** 2001. Molecular characterization of estuarine bacterial communities that use high- and low-molecular weight fractions of dissolved organic carbon. Aquat. Microbiol. Ecol. **25:**127–139.
10. **DeLong, E. F., D. G. Franks, and A. L. Alldredge.** 1993. Phylogenetic diversity of aggregate-attached vs. free-living marine bacterial assemblages. Limnol. Oceanogr. **38:**924–934.
11. **Falkowski, P. G., R. J. Scholes, E. Boyle, J. Canadell, D. Canfield, J. Elser, N. Gruber, K. Hibbard, P. Hogberg, S. Linder, F. T. Mackenzie, B. Moore III, T. Pedersen, Y. Rosenthal, S. Seitzinger, V. Smetacek, and W. Steffen.** 2000. The global carbon cycle: a test of our knowledge of Earth as a system. Science **290:**291–296.
12. **Finkelstein, D. A., L. M. Tender, and J. G. Zeikus.** 2006. Effect of electrode potential on electrode-reducing microbiota. Environ. Sci. Technol. **40:**6990–6995.
13. **Freguia, S., K. Rabaey, Z. Yuan, and J. Keller.** 2007. Electron and carbon balances in microbial fuel cells reveal temporary bacterial storage behavior during electricity generation. Environ. Sci. Technol. **41:**2915–2921.
14. **Froelich, P. N., G. P. Klinkhammer, M. L. Bender, N. A. Luedtke, G. R. Heath, D. Cullen, P. Dauphin, D. Hammond, B. Hartman, and V. Maynard.** 1979. Early
15. **Fujii, M., S. Murashige, Y. Ohnishi, A. Yuzawa, H. Miyasaka, Y. Suzuki, and H. Komiyama.** 2002. Decomposition of phytoplankton in seawater. I. Kinetic analysis of the effect of organic matter concentration. J. Oceanogr. **58:**433–438.
16. **Girguis, P. R., V. J. Orphan, S. J. Hallam, and E. F. DeLong.** 2003. Growth and methane oxidation rates of anaerobic methanotrophic archaea in a continuous-flow bioreactor. Appl. Environ. Microbiol. **69:**5472–5482.
17. **Harvey, H. R., J. H. Tuttle, and J. T. Bell.** 1995. Kinetics of phytoplankton decay during simulated sedimentation: changes in biochemical composition and microbial activity under oxic and anoxic conditions. Geochim. Cosmochim. Acta **59:**3367–3377.
18. **He, Z., S. D. Minteer, and L. T. Angenent.** 2005. Electricity generation from artificial wastewater using an upflow microbial fuel cell. Environ. Sci. Technol. **39:**5262–5267.
19. **Hee, C. A., T. K. Pease, M. J. Alperin, and C. S. Martens.** 2001. Dissolved organic carbon production and consumption in anoxic marine sediments: a pulsed-tracer experiment. Limnol. Oceanogr. **46:**1908–1920.
20. **Holmes, D. E., D. R. Bond, R. A. O'Neil, C. E. Reimers, L. R. Tender, and D. R. Lovley.** 2004. Microbial communities associated with electrodes harvesting electricity from a variety of aquatic sediments. Microb. Ecol. **48:**178–190.
21. **Ieropoulos, I. A., J. Greenman, C. Melhuish, and J. Hart.** 2005. Comparative study of three types of microbial fuel cell. Enzymol. Microbiol. Technol. **37:**238–245.
22. **Jeroschewski, P., C. Steuckart, and M. Kühl.** 1996. An amperometric microsensor for the determination of H_2S in aquatic environments. Anal. Chem. **68:**4351–4357.
23. **Jørgensen, B. B.** 2006. Bacteria and marine biogeochemistry, p. 169–206. *In* H. D. Schulz and M. Zabel (ed.), Marine geochemistry, 2nd ed. Springer, Berlin, Germany.
24. **Jørgensen, B. B., and F. Bak.** 1991. Pathways and microbiology of thiosulfate transformations and sulfate reduction in a marine sediment (Kattegat, Denmark). Appl. Environ. Microbiol. **57:**847–856.
25. **Kim, H. J., H. S. Park, M. S. Hyun, I. S. Chang, M. Kim, and B. H. Kim.** 2002. A mediator-less microbial fuel cell using a metal reducing bacterium, Shewanella putrefacians. Enzymol. Microbiol. Technol. **30:**145–152.
26. **Liu, H., and B. E. Logan.** 2004. Electricity generation using an air-cathode single chamber microbial fuel cell in the presence and absence of a proton exchange membrane. Environ. Sci. Technol. **38:**4040–4046.
27. **Liu, H., R. Ramnarayanan, and B. E. Logan.** 2004. Production of electricity during wastewater treatment using a single chamber microbial fuel cell. Environ. Sci. Technol. **38:**2281–2285.
28. **Liu, W.-T., T. L. Marsh, H. Cheng, and L. J. Forney.** 1997. Characterization of microbial diversity by determining terminal restriction fragment length polymorphisms of genes encoding 16S rRNA. Appl. Environ. Microbiol. **63:**4516–4522.
29. **Llobet-Brossa, E., R. Rosselló-Mora, and R. Amann.** 1998. Microbial community composition of Wadden Sea sediments as revealed by fluorescence in situ hydridization. Appl. Environ. Microbiol. **64:**2691–2696.
30. **Logan, B. E., B. Hamelers, R. Rozendal, U. Schröder, J. Keller, S. Freguia, P. Aelterman, W. Verstraete, and K. Rabaey.** 2006. Microbial fuel cells: methodology and technology. Environ. Sci. Technol. **40:**5181–5192.
31. **Lovley, D. R.** 2006. Microbial energizers: fuel cells that keep on going. Microbe **1:**323–329.
32. **Lovley, D. R., and E. J. P. Phillips.** 1987. Competitive mechanisms for inhibition of sulfate reduction and methane production in the zone of ferric iron reduction in sediments. Appl. Environ. Microbiol. **53:**2636–2641.
33. **McCartney, D. M., and J. A. Oleskiewicz.** 1991. Sulphide inhibition of anaerobic degradation of lactate and acetate. Water Res. **25:**203–209.
34. **Millero, F. J., T. Plese, and M. Fernandez.** 1988. The dissociation of hydrogen sulfide in seawater. Limnol. Oceanogr. **33:**269–274.
35. **Min, B., J. Kim, S. Oh, J. M. Regan, and B. E. Logan.** 2005. Electricity generation from swine wastewater using microbial fuel cells. Water Res. **39:**4961–4968.
36. **Ohnishi, Y., M. Fujii, S. Murashige, A. Yuzawa, H. Miyasaka, and Y. Suzuki.** 2004. Microbial decomposition of organic matter derived from phytoplankton cellular components in seawater. Microbes Environ. **19:**128–136.
37. **Pfenning, N., and H. Biebl.** 1976. *Desulfuromonas acetoxidans* gen. nov. and sp. nov., a new anaerobic, sulfur-reducing, acetate-oxidizing bacterium. Arch. Microbiol. **110:**3–12.
38. **Rabaey, K., P. Clauwaert, P. Aelterman, and W. Verstraete.** 2005. Tubular microbial fuel cells for efficient electricity generation. Environ. Sci. Technol. **39:**8077–8082.
39. **Rabaey, K., G. Lissens, S. D. Siciliano, and W. Verstraete.** 2003. A microbial fuel cell capable of converting glucose to electricity at high rate and efficiency. Biotechnol. Lett. **25:**1531–1535.
40. **Rabaey, K., K. Van De Sompel, L. Maignien, N. Boon, P. Aelterman, P. Clauwaert, L. De Schamphelaire, H. T. Pham, J. Vermeulen, M. Verhaege, P. Lens, and W. Verstraete.** 2006. Microbial fuel cells for sulfide removal. Environ. Sci. Technol. **40:**5218–5224.

41. **Redfield, A. C.** 1958. The biological control of chemical factors in the environment. Am. Sci. **46:**205–221.

42. **Reimers, C. E., P. Girguis, H. A. Stecher III, L. M. Tender, N. Ryckelynck, and P. Whaling.** 2006. Microbial fuel cell energy from an ocean cold seep. Geobiology **4:**123–136.

43. **Reimers, C. E., L. M. Tender, S. Fertig, and W. Wang.** 2001. Harvesting energy from the marine sediment-water interface. Environ. Sci. Technol. **35:**192–195.

44. **Roychoudhury, A. N., P. Van Cappellan, J. E. Kostka, and E. Violler.** 2003. Kinetics of microbially mediated reactions: dissimilitory sulfate reduction in saltmarsh sediments (Sapelo Island, Georgia, USA). Estuar. Coast. Shelf Sci. **56:**1001–1010.

45. **Ryckelynck, N., H. A. Stecher III, and C. E. Reimers.** 2005. Understanding the anodic mechanism of a seafloor fuel cell: interactions between geochemistry and microbial activity. Biogeochemistry **76:**113–139.

46. **Sørensen, J., D. Christensen, and B. B. Jørgensen.** 1981. Volatile fatty acids and hydrogen as substrates for sulfate-reducing bacteria in anaerobic sediment. Appl. Environ. Microbiol. **42:**5–11.

47. **Suess, E., and P. J. Müller.** 1980. Productivity sedimentation rate and sedimentary organic matter in the oceans. II. Elemental fractionation, p. 17–26. *In* Colloques Internationaux du C.N.R.S., 293. C.N.R.S., Paris, France.

48. **Tender, L. M., C. E. Reimers, H. A. Stecher III, D. E. Holmes, D. R. Bond, D. A. Lowy, K. Pilobello, S. J. Fertig, and D. R. Lovley.** 2002. Harnessing microbially generated power on the seafloor. Nat. Biotechnol. **20:**821–825.

49. **Westrich, J. T., and R. A. Berner.** 1984. The role of sedimentary organic matter in bacterial sulfate reduction: the G model tested. Limnol. Oceanogr. **29:**236–249.

50. **Winfrey, M. R., and D. M. Ward.** 1983. Substrates for sulfate reduction and methane production in intertidal sediments. Appl. Environ. Microbiol. **45:**193–199.

51. **Wirsen, C. O., S. M. Sievert, C. M. Cavanaugh, S. J. Molyneaux, A. Ahmad, L. T. Taylor, E. F. DeLong, and C. D. Taylor.** 2002. Characterization of an autotrophic sulfide-oxidizing marine *Arcobacter* sp. that produces filamentous sulfur. Appl. Environ. Microbiol. **68:**316–325.

52. **Zar. J. H.** 1984. Biostatistical analysis, 2nd ed. Prentice-Hall, Inc., Englewood Cliffs, NJ.